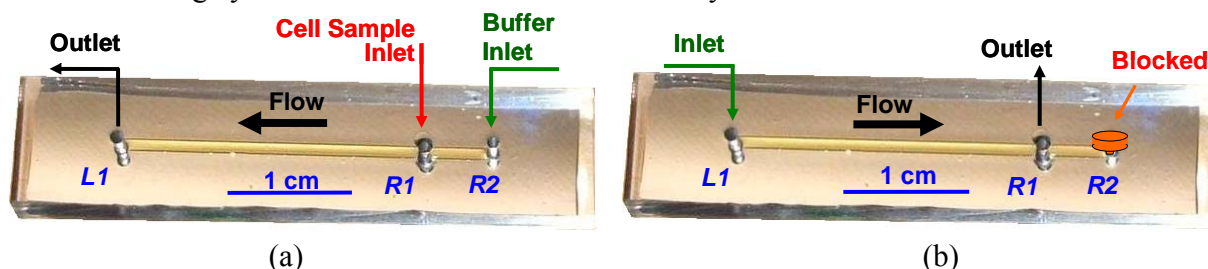


## Electronic Supplementary Information

### Experimental set-up for cell attachment and detachment

The attachment setup is shown in Figure 1a. The flow was driven from port *R2* to port *L1* using two syringe pumps (PhD 2000, Harvard Apparatus). A pipette tip, loaded with 50  $\mu\text{l}$  of buffer solution (1 $\times$ CMF-PBS) on top of 10  $\mu\text{l}$  of cell suspension ( $\sim 250$  cells/ $\mu\text{l}$ ), was inserted into port *R1*; the buffer solution was used for channel washing once all the sample cells entered the microchannel. Experiments started by turning on the pump at *R2*, applying pressure in a forward motion, with a programmed flow rate  $Q$  ranging between 0.3 and 3  $\mu\text{l}/\text{min}$ ; immediately after, the pump at *L1* was turned on applying suction in a backward motion with the same flow rate  $Q$ . The flow field reached a steady-state within 30 seconds and, thereafter, the flow rate imposed by the pump at *R2* was reduced by half from  $Q$  to  $Q/2$ . Consequently, conservation of mass dictated the establishment of flow from port *R1* at a rate of  $Q/2$  as well. Once cells enter the channel, they were carried away downstream by a steady flow allowing them to gradually sediment and interact with the functionalized channel bottom surface. The number of cells entering the microchannel  $N_0$  was counted, typically in the range of 2000-2500. Once the cell sample had been fully loaded, the channel was flushed with the 1 $\times$ CMF-PBS buffer solution, at a flow rate of 3  $\mu\text{l}/\text{min}$  for 3 minutes, to remove unbound cells while keeping captured target cells unaffected. The flow was then stopped, and 22 images along the entire microchannel were recorded to determine the total number of attached cells  $N_A$ .

In the detachment setup, shown in Figure 1b, the channel port *L1* was connected to a syringe pump to apply pressure in a forward motion. Port *R2* was blocked while leaving port *R1* open; thus, the flow rate from *L1* to *R1* was controlled by the single pump at port *L1*. All detachment experiments started with an attachment step, in which firm adhesion of the captured cells was established. In this step, each cell suspension was driven through a functionalized microchannel under a 0.5  $\mu\text{l}/\text{min}$  flow rate followed by a 3-minute-washing at a 3  $\mu\text{l}/\text{min}$  flow rate. The pumps were then turned off, and images of the captured cell population were recorded to determine the number of attached cells  $N_A$ . In the next detachment step, the flow direction was reversed increasing at a constant acceleration until reaching a prescribed flow rate. The pump was turned off after maintaining this prescribed flow rate for 5 min, and images of the remaining attached cells were recorded. The difference between the number of captured cells before and after the detachment stage yielded the number of cells removed by the flow  $N_D$ .



**Figure 1** Photographs of a packaged microfluidic device depicting the connections to the external fluid handling systems for: (a) cell attachment; where two syringe pumps are connected to ports *L1* and *R2*, respectively, with port *R1* used for cell sample loading (flow is right-to-left), and (b) cell detachment; where the syringe pump is connected to port *L1*, with port *R2* blocked, leaving port *R1* as the outlet (flow is left-to-right). The microchannel is about 100  $\mu\text{m}$  high and 1 mm wide; the length between *R1* and *L1* is about 25 mm.

The current microdevice consisting a single microchannel allows processing of about 10 $\mu$ l cell sample (up to about 2500 cells), and this is clearly not sufficient for practical use. However, the flexibility of the microfluidic channel approach offers an easy solution to improve the throughput. A microchannel array rather than a single microchannel can be used along with a greater channel height. Using a microdevice comprising an array of 10 microchannels, each about 200 $\mu$ m in height, a sample solution on the order of 1-10ml can be processed under the same published flow protocol before losing cell viability; this is an acceptable throughput even for clinical applications.

### Cell sedimentation time and distance

In the current experimental set-up, video recording of cells inside a microchannel was accomplished using a top-view camera. This arrangement enabled excellent tracking of in-plane cell motion but made it difficult to resolve the vertical out-of-plane motion. In particular, the precise instant and location of a cell first contact with the functionalized surface could not be determined. An estimate of the average sedimentation time and distance was obtained in a separate experiment. The settling motion of several cells in a glass capillary filled with 1 $\times$ CMF-PBS buffer solution was recorded using a side-view camera. The terminal velocity of each cell was measured from the recorded images, and the average cell terminal velocity was found to be about 10 $\mu$ m/s. Thus, a time interval of 5s was needed for an average cell to traverse half the channel height, i.e. 50 $\mu$ m, from its entry into the microchannel until complete sedimentation. The average sedimentation distance was estimated from flow-rate dependent average cell velocity prior to sedimentation. For example, under a flow rate of 0.5 $\mu$ l/min, the population average cell velocity around the channel inlet was measured to be about 100 $\mu$ m/s yielding an estimated sedimentation distance of about 500 $\mu$ m.

### Attachment kinetics of cell capture in bio-functionalized microchannels

A simplified attachment kinetics model has been proposed to analyze receptor mediated cell-surface interaction as a simple chemical reaction [1]. Based on this model, the accumulated number of captured cells  $N_B$  obeys a first-order rate law [2, 3]. Utilizing the averaged cell velocity  $U_C$  for scaling, the accumulated number of captured cells can be rewritten as a spatial rather than temporal function [2]:

$$\frac{dN_B(x)}{dx} = \frac{k_{ad}}{U_C} [N_A - N_B(x)] \quad (1)$$

where  $k_{ad}$  is the adhesion rate constant, and  $N_B(x)$  is the spatial distribution of bound cells along the channel. The adhesion rate constant can be extracted from the observed spatial distribution of captured cells along the channel. Equation 1 can be integrated to yield an analytical solution for  $N_B(x)$  [2]. However, this approximation requires that all cells be in contact with the channel bottom surface while, in the experiments, the cells travel a certain distance  $x_S$  before contacting the channel surface. Accounting for this sedimentation distance, the solution for Equation 1 is:

$$\frac{N_B(x)}{N_A} = 1 - \exp\left[-\frac{k_{ad}}{U_C}(x - x_S)\right] \quad (2)$$

On average, given the cell settling velocity of 10 $\mu$ m/s and channel height of 100 $\mu$ m, it takes about 5s for cells to complete their sedimentation from the channel mid-height level. The downstream distance travelled by cells during this 5s sedimentation time depends on the applied flow rate; for a rate of 0.5 $\mu$ l/min, the sedimentation distance is estimated to be about  $x_S=500\mu$ m.

Although a first-order kinetics model may not adequately describe non-specific cell-surface interactions, we use it here to highlight the difference between specific and non-specific cell-surface binding. The accumulated numbers of attached MDA-MB-231 and BT-20 cells in anti-cadherin-11 functionalized microchannels were counted for a flow rate of  $0.5\mu\text{l}/\text{min}$  ( $U_c=45.4\mu\text{m}/\text{s}$ ). The measured results and predictions based on Equation 2 are plotted in Figure 2 as a function of the normalized distance along the channel. Clearly, the model calculations fit the experimental data for the cadherin-11-expressing MDA-MB-231 cells far better than for the non-expressing BT-20 cells; nonetheless, the model-based estimations of the adhesion-rate constants for the MDA-MB-231 and BT-20 cells are  $k_{ad}=0.027\text{s}^{-1}$  and  $0.0045\text{s}^{-1}$ , respectively.

The spatial distribution of captured cells can be described more accurately by a lognormal statistical model because: (i) the cell-surface binding depends on several independent and random variables, such as the probabilistic nature of bond formation and rupture, and (ii) the distance travelled by cells from the channel inlet to the resting location is positive definite. The cumulative distribution function of such a lognormal distribution is given by:

$$f\left(\frac{x}{L}\right) = \frac{1}{2} + \frac{1}{2} \operatorname{erf}\left[\frac{\ln(x/L) - \mu}{\sigma_A \sqrt{2}}\right] \quad (3)$$

where  $\mu$  and  $\sigma_A$  are respectively the mean and standard deviation of the natural logarithm of the normalized location of captured cells, i.e.  $X=x/L$ . Denoting the location for the median of  $f(X)$  as  $X_M$ , such that  $f(X=X_M)=0.5$ , Equation 3 can be re-written as:

$$f(X) = \frac{1}{2} + \frac{1}{2} \operatorname{erf}\left[\frac{\ln(X/X_M)}{\sigma_A \sqrt{2}}\right] \quad (4)$$

One expects the two fitting parameters,  $X_M$  and  $\sigma_A$ , to be smaller for cell-surface specific binding. The best-fit curves are graphed in Figure 2 where, at least for the specific binding of MDA-MB-231, the lognormal distribution faithfully traces the experimental results along the entire microchannel. The fitting parameters are  $X_M=0.08$  and  $0.3$  with  $\sigma_A=1.3$  and  $1.9$  for MBA-MB-231 and BT-20 cells, respectively. Indeed, the specific binding of cadherin-11-expressing MDA-MB-231 cells in an anti-cadherin-11-functionalized microchannel features a smaller median distance and standard deviation indicating an interaction with much higher affinity and less randomness compared with the non-specific binding of BT-20 cells.

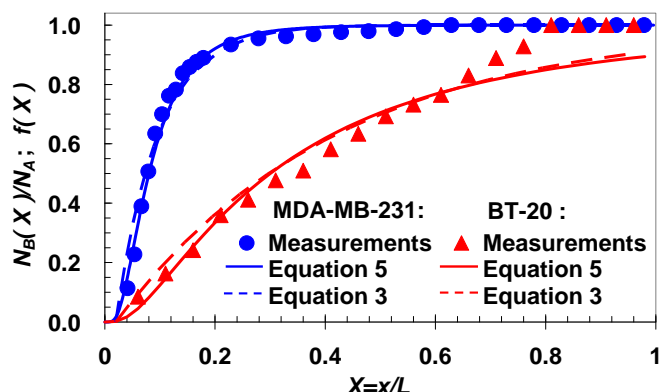


**Figure 2** A comparison of measured accumulated number of captured MDA-MB-231 and BT-20 cells along anti-cadherin-11 functionalized microchannels with curves calculated based on the 1st-order chemical-reaction model (Eq. 2) and the lognormal statistical model (Eq. 4).

## References

- 1 C. Cozens-Roberts, J. A. Quinn, and D. A. Lauffenberger, Receptor-mediated cell attachment and detachment kinetics. II. Experimental model studies with the radial-flow detachment assay. *Biophys. J.*, **vol. 58**, pp. 857-872, 1990.
- 2 D. G. Swift, R. G. Posner, and D. A. Hammer, Kinetics of adhesion of IgE-sensitized rat basophilic leukemia cells to surface-immobilized antigen in Couette flow. *Biophys. J.*, **vol. 75**, pp. 2597-2611, 1998.
- 3 A. Sin, S. K. Murthy, A. Revzin, R. G. Tompkins and M. Toner, Enrichment using antibody-coated microfluidic chambers in shear flow: Model mixtures of human lymphocytes. *Biotechnol. Bioeng.*, **vol. 91**, pp. 816-826, 2005.